Warm-to-Cold Water Conversion in the Northern North Atlantic Ocean[1]

M. S. McCARTNEY AND L. D. TALLEY[2]

Woods Hole Oceanographic Institution, Woods Hole, MA 02543

(Manuscript received 22 April 1983, in final form 21 February 1984)

ABSTRACT

A box model of warm-to-cold-water conversion in the northern North Atlantic is developed and used to estimate conversion rates, given water mass temperatures, conversion paths and rate of air–sea heat exchange. The northern North Atlantic is modeled by three boxes, each required to satisfy heat and mass balance statements. The boxes represent the Norwegian Sea, and a two-layer representation of the open subpolar North Atlantic. In the Norwegian Sea box, warm water enters from the south, is cooled in the cyclonic gyre of the Norwegian–Greenland Sea, and the colder water returns southwards to the open subpolar North Atlantic. Some exchange with the North Polar Sea also is included. The open subpolar North Atlantic has two boxes. In the abyssal box, the dense overflows from the Norwegian Sea flow south, entraining warm water from the upper-ocean box. In the upper-ocean box, warm water enters from the south, supplying the warm water for an upper ocean cyclonic circulation that culminates in production by convection of Labrador Sea Water, and also the warm water that is entrained into the abyss, and the warm water that continues north into the Norwegian Sea. Our estimates are that 14×10^6 m^3 s^{-1} of warm (11.5°C) water flows north to the west of Ireland, with about a third of this branching into the Norwegian Sea. The production rate for Labrador Sea Water is 8.5×10^6 m^3 s^{-1}, and this combines with a flow of dense Norwegian Sea Overflow waters (with entrained warmer waters) at 2.5×10^6 m^3 s^{-1} to give a Deep Western Boundary Current of 11×10^6 m^3 s^{-1}. The total southward flow east of Newfoundland is this plus 4×10^6 m^3 s^{-1} of cold less dense Labrador Current waters (there is a net southward flow between Newfoundland and Ireland of about 1×10^6 m^3 s^{-1} supplied by northward flow through the Bering Strait, passing through the North Polar Sea to enter the Norwegian Sea.

1. Introduction

The advection of warm water to high latitudes by poleward flowing surface currents carries with it the potential for production of intermediate and deep water masses by air–sea interaction. If the net buoyancy flux at the sea surface is negative, then convective overturning can occur and produce denser products. A net negative buoyancy flux occurs when the cooling of warm water and the concomitant salt flux due to evaporation is strong enough to give a negative buoyancy flux at the sea surface of magnitude greater than the positive buoyancy flux due to fresh water input by precipitation and run-off. Convection vertically homogenizes the water column to some depth (depending on the underlying pycnocline structure and therefore on both the local time history of buoyancy flux through the sea surface and the history of buoyancy flux along advection paths to the location in question). The impact of the homogeneous product on ocean water masses depends on its volume (depth of the convection times area over which convection occurs) and the rate at which the homogeneous water is produced. The regional impact will be determined by the advection paths carrying the product away from the convection region.

A description of upper-ocean convection in the Subpolar North Atlantic was given by McCartney and Talley (1982), and Fig. 1 includes a chart of the temperature of the winter deep mixed layer from that study. The North Atlantic Current carries warm water northwards near the western boundary, east of Newfoundland. Along the right hand side of the Current deep convection occurs, producing pycnostads of temperatures between 15 and 10°C as can be seen in section 2a in Fig. 2. In this section, the northward flowing Current is crossed near 40°W, and east of there is a broad zone of Subpolar Mode Water. Near 50°N this Current turns offshore and extends eastward across the North Atlantic. In the general neighborhood of the eastern end of section 2a, there is a bifurcation of the eastern flow into northward and southward branches. Some of the Subpolar Mode Water recirculates southwards in the subtropical anticyclonic gyre (McCartney, 1982). The rest turns northwards near the eastern boundary of the North Atlantic, west of Ireland, as can be seen in section 2b (Fig. 2). The Subpolar Mode Water pycnostad lies above the tilted thermocline that

[1] Woods Hole Oceanographic Institution Contribution Number 5410.

[2] Present affiliation: Scripps Institution of Oceanography, La Jolla, CA 92037.

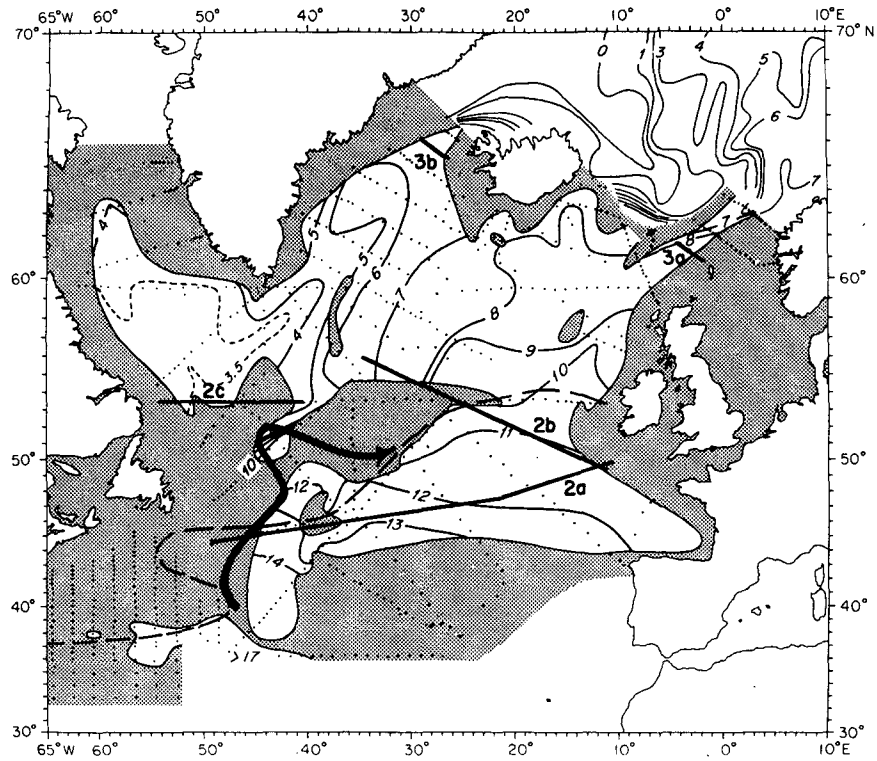

FIG. 1. Potential temperature θ (°C) of the surface mixed layer of the subpolar North Atlantic in late winter—January–April. θ is contoured only where the thickness of a surface or near-surface density layer of $\Delta\sigma_\theta = 0.02$ mg cm^{-2} exceeds 200 m. The shaded area represents the region where this thickness is less than 200 m. Except for part of the Norwegian Current, the Norwegian Sea is excluded from this contouring. This part of the figure was previously published by McCartney and Talley (1982). In the Norwegian Sea the 200 m "winter" temperature field from Dietrich (1969) has been reproduced. The heavy dashed contour is the contour of zero annual mean wind-stress curl from Leetmaa and Bunker (1978); linear wind-driven circulation theory gives cyclonic circulation north of this contour and anticyclonic circulation south of it. The North Atlantic Current is shown as a heavy solid curve. Lines 2a, b and c, and 3a and b give section locations used in Figs. 2 and 3. Sections 2c, 3a and 3b were used in the contouring of this chart, 2a and 2b were not. See text for further discussion.

marks the northward branch of the North Atlantic Current. Saunders (1982) has estimated a northeastward transport of 18×10^6 m^3 s^{-1} above 800 m in section 2b, which is a warm water source for the subpolar North Atlantic. This source is volumetrically dominated by the local Mode Water at 11°C. This warm water is made colder and denser by heat loss along two main paths, one in the open subpolar North Atlantic and the second in the Norwegian Sea.[3] In the first the warm water is cooled along the counterclockwise path from about 11°C in the east to below 4°C in the Labrador Sea. The coldest (and densest and freshest) mixed layers occur in the Labrador Sea, and we have identified these deep convectively formed pycnostads as Labrador Sea Water. Section 2c (Fig. 2) illustrates a winter section from the Labrador Sea with the pycnostad layer open to the atmosphere just offshore of the cold and very fresh Labrador Current at 53°N. Using the low potential vorticity character of the pycnostad, the Labrador Sea Water influence can be tracked well south, as part of the Deep Western Boundary Current (Talley and McCartney, 1982). On the western end of section 2a, at 44°N, the low potential vorticity layer can be seen intruding southwards inshore of and beneath the North Atlantic Current, completely cut off from atmospheric contact. In the abyss of the western ends of both sections 2a and 2c, the cold dense Norwegian Sea Overflows can be seen wending their way southwards. The shallower Labrador Sea Water is part of this Deep Western Boundary Current structure.

The second circulation path starts as a branch from the subpolar North Atlantic cyclonic gyre into the Norwegian Sea. Fig. 3 shows temperature sections from

[3] In the remainder of this paper, the open North Atlantic north of 50°N and south of Baffin Bay and the Norwegian–Greenland Seas will be called the subpolar North Atlantic. The Norwegian–Greenland Sea will be simply called the Norwegian Sea, after Worthington (1970).

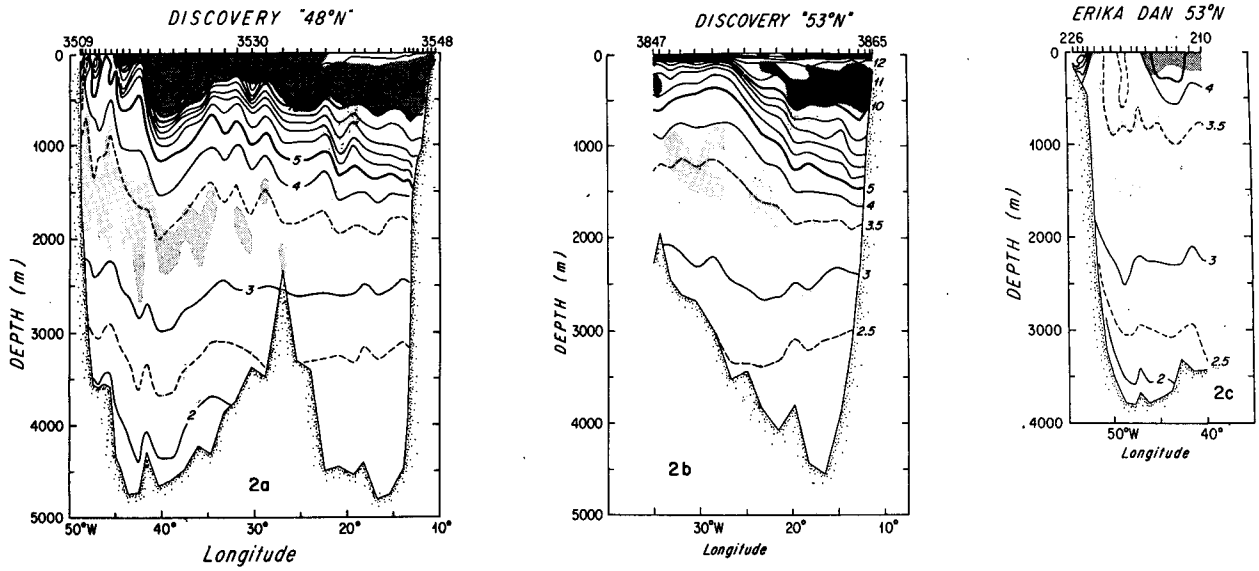

FIG. 2. Potential temperature (°C) sections illustrating the major flows past 50°N (nominal, see Fig. 1 for sections). Heavy shading indicates the layer with potential vorticity less than 75×10^{-14} cm^{1} s^{-1} that forms the core layer of the Subpolar Mode Water (McCartney and Talley, 1982). Light shading indicates the layer of very low potential vorticity—less than 8×10^{-14} cm^{-1} s^{-1} that forms the core layer of the Labrador Sea Water (Talley and McCartney, 1982). The *Discovery* 48°N section (section 2a) was made in Spring 1957, the 53°N section (section 2b) in August 1958. The *Erika Dan* 53°N section (section 2c) was made in February 1962. See the text for discussion.

the Faroe–Shetland Channel and the Denmark Strait. The local Mode Waters, at temperatures warmer than 8 and 6°C, respectively, overlie much colder Norwegian Sea outflows. Entrainment across this strong temperature front undoubtedly is a major contributor to the downstream increase in temperature and transport of the cold dense Norwegian Sea overflows (Worthington, 1970). The 8°C water at Faroe–Shetland channel seems to be the main warm inflow to the Norwegian Sea. Further air–sea exchanges along the Norwegian Current, and the cyclonic gyre of the Norwegian Sea, convert this warm water to cold dense water masses (Swift *et al.*, 1980; Swift and Aagaard, 1981). The warm water flowing northwards through Denmark Strait to feed the North Icelandic Irminger Current (Stefánsson, 1962) seems a less important warm source.

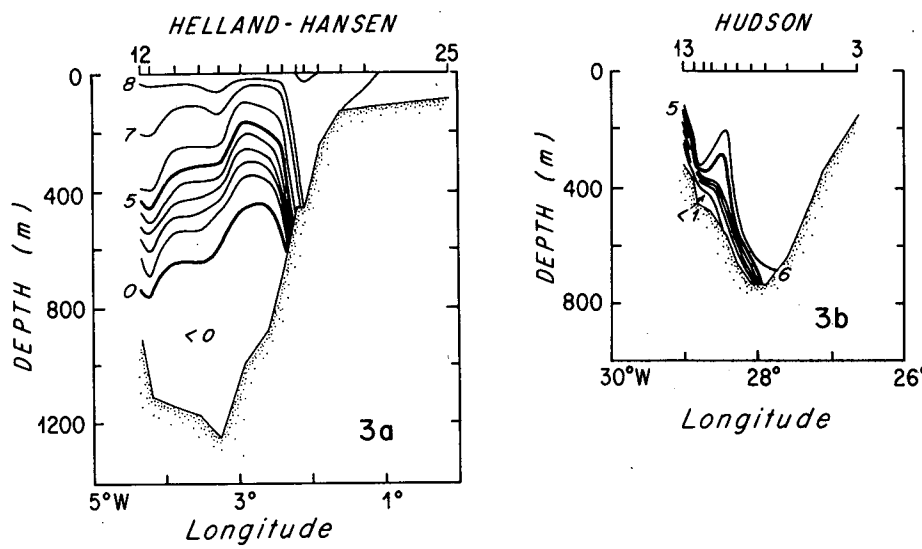

FIG. 3. Sections of potential temperature near (3a) Faroe–Shetland Channel and (3b) Denmark Strait. See Fig. 1 for locations.

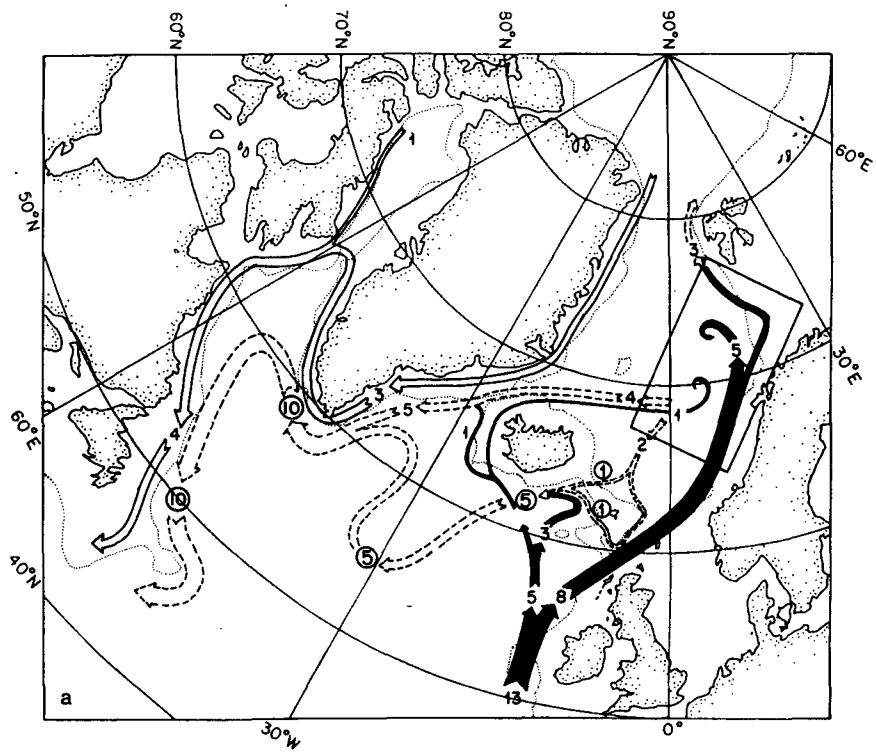

FIG. 4. Water mass conversion flow paths, Norwegian Sea and subpolar North Atlantic.
(a) Worthington's (1970) published scheme for the Norwegian Sea, and the overflows into entrainments within the subpolar basin. Warm (>4°C) currents are black, dense cold (<4°C) overflows dashed, and light cold overflows unshaded. The curled ends to the warm currents denote sinking across 4°C.
(b) A modification of Worthington's (1970) scheme based on his later box model (1976). The modifications include formation of Labrador Sea Water (sinking below 4°C), a recirculation of 4×10^6 m^3 s^{-1} of the Deep Western Boundary Current, and a subpolar upwelling of Labrador Sea water and Deep Western Boundary Current water into the thermocline layer.
(c) Our proposal for further modification to Worthington's scheme (Figs. 4a and 4b). The warm water flowing northwards is partially utilized for a net production of Labrador Sea water. For purposes of a box model north of 50°N, recirculations (as in Fig. 4b) are treated as internal modes that don't effect the net heat budget, and have been dropped for clarity. The direct participation of Labrador Sea Water in the Deep Western Boundary current is indicated by the dashed bifurcation in this current. Fig. 5 shows a schematic of the resulting idealized box model.

The cold dense overflows (Fig. 3) from the Norwegian Sea entrain warmer waters all along their path down the western boundaries of basins. At 50°N the temperature has risen from the <0°C value within the Norwegian Sea to a level of about 2°C (Worthington, 1970). Additional cold but very fresh and light water makes its way southwards at the western edge of the sea surface. This current (East and West Greenland and Labrador Currents) is characterized by a temperature near 0°C (it can be seen in the upper water on the western ends of sections 2a, 2c and 3b).

There is some literature on estimates of the volume fluxes of some elements of the above system. Worthington (1970) reviewed direct measurements of the dense overflows from the Norwegian Sea; his summary circulation diagram is shown as Fig. 4a. In this figure, the circled transport numbers represent "measured" values—dynamic computations with Swallow-float based reference-level velocities. His system shows a northward transport of warm water of 13×10^6 m^3 s^{-1}, with a return flow across 50°N of 10×10^6 m^3 s^{-1} in the dense water of the Deep Western Boundary Current, and 4×10^6 m^3 s^{-1} of light cold water in the Labrador Current (the net southward flow of 1×10^6 m^3 s^{-1} comes from the North Pacific via the North Polar Sea).

The transport scheme shown in Fig. 4a carries with it a requirement of heat loss from the ocean to the atmosphere in the Norwegian Sea. Using the illustrated transports and estimates of the temperatures of the mean currents, Worthington (1970) found a loss of 63×10^{12} cal s^{-1}. Bunker's later computations of air–sea heat exchange (summarized by Bunker, 1976; amended by Bunker and Goldsmith, 1979; and archived at the Woods Hole Oceanographic Institution) were based on bulk aerodynamic formulas, and for this region

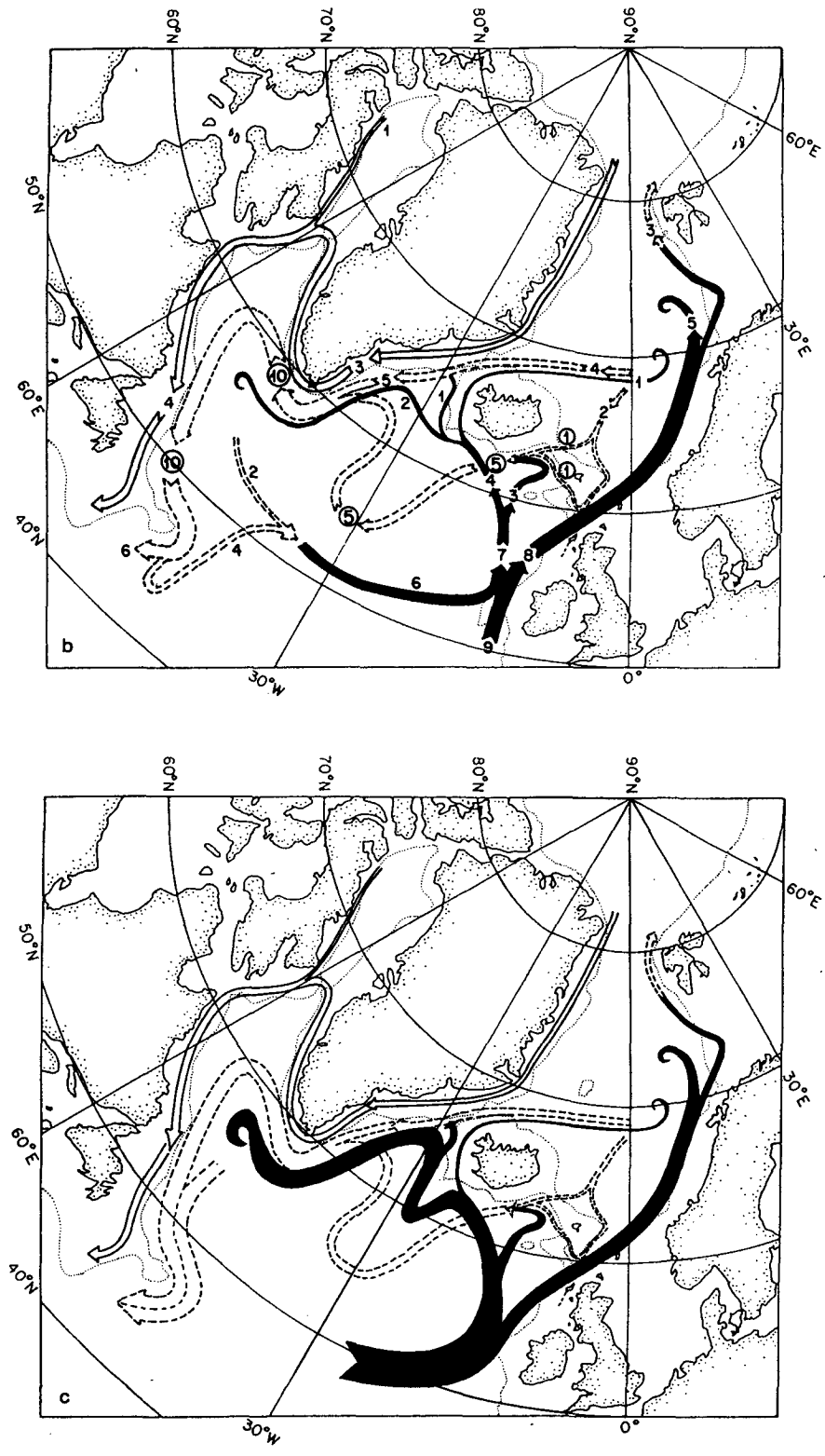

FIG. 4. (*Continued*)

give a long-term annual average of only half this, 31×10^{12} cal s^{-1}. Many possibilities could explain this difference, some of those being:

1) systematic error in Bunker formulation (see Talley, 1984, for a recent overview of some of the recent literature);

2) systematic bias in the data Bunker used (ships evading high winds and cold air outbreaks, not taking measurements in severe conditions);

3) nonrepresentativeness of the Worthington transport values (perhaps transport measurements were taken in particular years with higher-than-average formation rates, for example).

Another possibility involves the nature of the abyssal circulation (see Stommel and Arons, 1960). The southward transport in a Deep Western Boundary Current at a given latitude is not simply given by the high-latitude source strength less that lost north of that latitude by upwelling. The Current is augmented by recirculation in steady abyssal cyclonic gyres driven by upwelling into the thermocline. This augmentation can be large. As an example, Stommel and Arons (1960) discuss a pie-shaped basin in a sphere. With a source at the pole of strength S_0, and a basin bounded by two meridians of longitude and the equator, the deep westward boundary current transport is $2S_0 \times \sin\theta$, where θ is latitude. Thus, at high latitudes the western intensified southward transport is nearly twice the source strength. In Fig. 4a, the only measured transports, the circled 5s and 10s, presumably then include local basin recirculations of unknown amounts. If it were the nearly doubling effect described by Stommel and Arons (1960), then the actual overflows would be half the amount indicated by Fig. 4a, and the implied heat flux would then agree with Bunker's numbers.

Worthington (1976) discussed a layered box model for the North Atlantic south of the Norwegian Sea. Based on his discussion, we have, in Fig. 4b, updated his 1970 chart with his estimations of the water mass conversions from the subpolar North Atlantic, the Norwegian Sea being unchanged. There are two main changes from the earlier model. First, there is an estimated 2×10^6 m^3 s^{-1} of Labrador Sea water sinking below 4°C in the west but upwelling farther east within the region north of 50°N. That is, it does not flow south past 50°N. Second, there is the immediate recirculation back northwards past 50°N of 40 percent of the southward transport of the Deep Western Boundary Current, and upwelling of this water into the overlying 4–7° layer. Thus, his estimated net flow of 2°C water south past 50°N has been reduced from 10 to 6 ($\times 10^6$ m^3 s^{-1}). There is also a hidden requirement of further production of Labrador Sea Water, since the warming of 6×10^3 m^3 s^{-1} of 1°C overflow water to 10×10^6 m^3 s^{-1} of 2°C water requires an entrainment of 4×10^6 m^3 s^{-1} of 3.5°C water for mass and heat consistency. Thus, the net flow of 6×10^6 m^3 s^{-1} of 2°C water has mixed within it 2.4×10^6 m^3 s^{-1} of Labrador Sea Water.

Worthington did not calculate the heat flux for the subpolar basin implied by either the 1970 or 1976 published schemes. In Table 1 we do, following the layout of his similar table for the Norwegian Sea in the 1970 paper. The Bunker numbers for this region add up to 87×10^{12} cal s^{-1}. The earlier Worthington (1970) scheme, Fig. 4a, carries an implied heat flux of 53×10^{12} cal s^{-1}; i.e., 60% of the Bunker value. The later box model, Worthington (1976), Fig. 4b, implies a heat flux of only 24×10^{12} cal s^{-1}; i.e., only 27% of the Bunker value.

The large discrepancy of heat flux between Bunker's estimate and the later model implies that a major water mass conversion process was omitted from Worthington's (1976) box model. This could be a larger net

TABLE 1. Subpolar North Atlantic heat budget—Worthington's 1970 system (see Fig. 4a).

	volume transport × temperature → heating rate (cm^3 s^{-1})	(°C)	(cal s^{-1})
Heat out			
Denmark Strait	1×10^{12}	6°	6×10^{12}
Faroe–Shetland Channel	8×10^{12}	9°	72×10^{12}
Deep Western Boundary Current	10×10^{12}	2°	20×10^{12}
			98×10^{12}
Heat in			
Eastern Atlantic Northward Flow	13×10^{12}	11°	143×10^{12}
Denmark Strait Overflow	4×10^{12}	1°	4×10^{12}
Iceland–Scotland Ridge Overflow	2×10^{12}	1°	2×10^{12}
			149×10^{12}
Heat loss to atmosphere = 53×10^{12} cal s^{-1}			
Same system modified to include Worthington's (1976) box model (see Fig. 4b).			
Heat out			
Denmark Strait	1×10^{12}	6°	6×10^{12}
Faroe–Shetland Channel	8×10^{12}	9°	72×10^{12}
Deep Western Boundary Current	10×10^{12}	2°	20×10^{12}
			98×10^{12}
Heat in			
Eastern Atlantic Northward Flow	9×10^{12}	12°	108×10^{12}
Recirculated Deep Western Boundary Current	4×10^{12}	2°	8×10^{12}
Denmark Strait Overflow	4×10^{12}	1°	4×10^{12}
Iceland–Scotland Ridge Overflow	2×10^{12}	1°	2×10^{12}
			122×10^{12}
Heat loss to atmosphere 122×10^{12} cal s^{-1} − 98×10^{12} cal s^{-1} = 24×10^{12} cal s^{-1}			

flow of Labrador Sea water south of 50°N. Our suggested modification to the Worthington (1976) model is to have more warm water flowing northwards past 50°N in the east, and a net southward flow of Labrador Sea water in the west adding to the southward flow of the Deep Western Boundary Current. Fig. 4c illustrates this modification. The Deep Western Boundary Current is modeled with two distinct components: the cold Norwegian Sea Overflow waters and the somewhat warmer Labrador Sea water.

In the next section a simple three-box model is developed that reflects the major elements of water mass conversion that occur in the Subpolar North Atlantic and Norwegian Sea. Temperatures of water masses are assigned from observation, but a number of production rates are treated as unknown. The system is forced by prescribed air–sea heat exchange, and each box is required to satisfy heat and mass conservation statements. The Bunker heat fluxes are used for the prime calculation, but other values as well as other temperature specifications are considered. The third section discusses the salinity balances required for consistency with the box model. The paper concludes with a discussion of other methods for estimating formation rates and of implications of the present study for the general circulation of the North Atlantic.

2. Box model for water mass conversion

The conversion rates of Subpolar Mode Water to Labrador Sea Water and Norwegian Sea Overflow water are estimated by approximating the different regions as layers with inflows and outflows of prescribed temperatures (from observations) and with specified heat loss to the atmosphere. The transport estimates for the inflows and outflows then can be estimated by requiring heat and mass balance statements to be satisfied for each layer. The transport magnitudes are those necessary to support the heat loss given the temperature differences between inflows and outflows. The Norwegian Sea is modeled with a single layer, while the subpolar North Atlantic is modeled with two layers in order to include the process of entrainment of warm water by the Norwegian Sea Overflow. A schematic of the box model is shown in Fig. 5. It is a simplified version of the circulation pattern illustrated in Fig. 4c.

Latitude 50°N is chosen as the southern boundary for the area of the box model because it is north of the location where the North Atlantic Current turns offshore, yet south of the main east-to-west flow of the subpolar cyclonic circulation. At 50°N, the pycnostad distribution indicates a northward flow of warm water in the east, dominated by the 11.5°C pycnostad (Fig. 1), and a southward flow of cool water in the west. There are two additional reasons to choose this latitude. First, Saunders (1982) has analyzed the upper circulation of the eastern North Atlantic. He found a bifurcation of the eastward North Atlantic Current into northward and southward branches in the neighborhood of 50°N. Second, the wind stress curl is zero near 50°N (Leetmaa and Bunker, 1978; see Fig. 1). This latitude marks the theoretical boundary between the subtropical anticyclonic circulation and the subpolar cyclonic circulation. Computation of the water

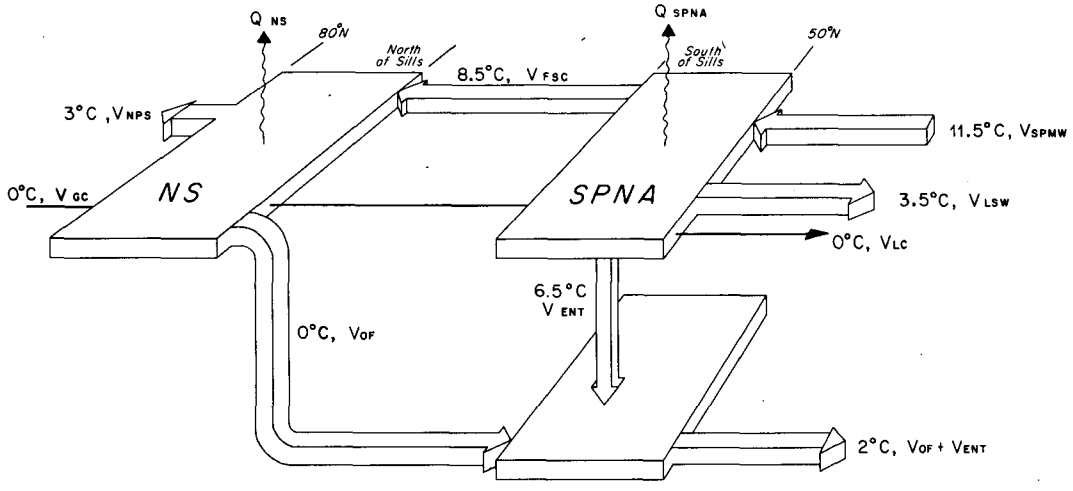

FIG. 5. Box model for the subpolar North Atlantic between 50 and 80°N, with a division at the Greenland–Scotland Ridge. The Norwegian Sea (NS) is treated as a single layer losing heat at the rate Q_{NS} to the atmosphere, with inflows and outflows of the indicated temperature. The remaining part of the subpolar North Atlantic (SPNA) is treated as two layers. The upper-layer loses heat at a rate Q_{SPNA} to the atmosphere, and loses water downwards at a rate V_{ENT} through entrainment into the lower layer. The upper layer exchanges water with the subtropical regime south of 50°N, and the Norwegian Sea to the north, at the indicated temperature. The lower layer receives water from dense Norwegian Sea overflows, and entrainment from the upper layer. The product of this mixture continues southwards past 50°N as a deep western boundary current.

mass conversion rate north of 50°N, therefore, will be an estimate of the net exchange of warm and cold water between the cyclonic and anticyclonic circulation, a thermohaline circulation superimposed on the wind-driven gyres.

The Subpolar Mode Water (SPMW) flowing from the south into the warm layer of the subpolar North Atlantic (V_{SPMW}) has a temperature of about 11.5°C (from Fig. 1).[4] This northward flow divides, with a branch (V_{FSC}) passing through the Faroe–Shetland Channel into the Norwegian Sea at a temperature of about 8.5°C (Fig. 3a). We choose to ignore the small contribution of warm water to the Norwegian Sea via the Denmark Strait, discussed in the preceding section. The rest of the Subpolar Mode Water is either entrained into the cold overflow water along the northern and western boundary of the subpolar North Atlantic (V_{ENT} at 6.5°C)[5] or is cooled along the cyclonic circulation path to become Labrador Sea Water (V_{LSW} at 3.5°C). The Labrador Sea Water is advected southwards along the western boundary as discussed in the preceding section.

The warm water flowing into the Norwegian Sea (V_{FSC}) provides the warm core of the Norwegian Current. This core is cooled and modified within the Norwegian Sea. Some of this current leaves the Sea to the north through the Spitzbergen–Greenland passage and enters the North Polar Sea (V_{NPS}), typically at a temperature of 3.0°C. In return the North Polar Sea provides a cold current back to the Norwegian Sea (V_{GC}) at a temperature of 0.0°C. It has been estimated that there is a net southward flow at the Spitzbergen–Greenland passage of 1×10^6 m^3 s^{-1} (Worthington, 1970, 1976), for which its ultimate source is the Pacific Ocean via the Bering Strait (Coachman and Aagaard, 1974). After Worthington (1970, 1976) we assume that the cold current along Greenland passes unaltered southwards to 50°N, i.e., that the temperature (0.0°C) and transport (4×10^6 m^3 s^{-1}) of the East and West Greenland and Labrador Currents remain fixed.

The rest of the warm water within the Norwegian Sea is cooled along the cyclonic circulation path to become mid-depth Arctic waters. Part of this progression can be seen in Fig. 1, where the winter 1958 temperature field at 200 m has been included in the Norwegian Sea, after Dietrich (1969). These cooled waters return to the subpolar North Atlantic as cold, dense overflows through the Faroe Bank Channel, over the Iceland–Faroe Ridge, and through the Denmark Strait. We lump these together as a single cold overflow (V_{OF}), at 0.0°C, and choose to ignore the multiple path aspect shown in Fig. 4. The overflow water appears to originate from the intermediate depth water mass of the Norwegian Sea, a convectively formed water mass near 0.0°C (Swift *et al.*, 1980; Swift and Aagaard, 1981).

The overflow waters enter the deep layer of the subpolar North Atlantic, and entrain warm water along the way. We model the entrainment as a volume transfer V_{ENT} from the upper to the lower layer of the Subpolar region. The entrainment temperature is chosen from the Denmark Strait overflow region, the apparent largest component of V_{OF}. Here the entraining water is the local Mode Water at 6.5°C (Fig. 3b). Farther downstream the entrainment temperature is probably lower. Indeed, Worthington's (1970) system shown in Fig. 4a actually uses a temperature of 3.5°C for the 4×10^6 m^3 s^{-1} of water that warms the 6×10^6 m^3 s^{-1} of 1°C water to 10×10^6 m^3 s^{-1} of 2° water ($6 \times 1° + 4 \times 3.5° = 10 \times 2°$). Our results depend somewhat on this temperature so at the end of this section we will report the results for 3.5°C. At 50°N the core temperature is about 2°C (Figs. 2a and 2c) and the transport is the sum of V_{OF} and V_{ENT}.

The annual heat losses from the ocean to the atmosphere in the two regions are denoted by Q_{NS} and Q_{SPNA}. The numbers used are 31×10^{12} cal s^{-1} and 87×10^{12} cal s^{-1}, respectively, obtained from unpublished tables by the late A. Bunker, made according to the methods described by Bunker (1976). An infrared correction has been applied, as discussed by Bunker and Goldsmith (1979). Alternate values for heat fluxes will be examined at the end of this section.

This completes the specification of the model. In the two regions we require balances of volume transport and heat transport, which can be written as follows. We arrange these equations with the prescribed quantities on the right-hand side, and the unknown transport terms to be determined on the left.

Norwegian Sea

$$\text{Volume:} \quad V_{FSC} - V_{OF} = V_{NPS} + V_{GC} - V_{GC}$$

$$\text{Heat:} \quad (8.5)V_{FSC} - (0.0)V_{OF} = \frac{Q_{NS}}{\rho c} + (3.0)V_{NPS} + (0.0)V_{GC} - (0.0)V_{GC}$$

Subpolar North Atlantic, upper layer

$$\text{Volume:} \quad V_{SPMW} - V_{FSC} - V_{LSW} - V_{ENT} = V_{GC} - V_{LC}$$

$$\text{Heat:} \quad (11.5)V_{SPMW} - (8.5)V_{FSC} - (3.5)V_{LSW} - (6.5)V_{ENT} = \frac{Q_{SPNA}}{\rho c} + (0.0)V_{GC} - (0.0)V_{LC}$$

[4] In addition to a simplified treatment of the exchanges between the Norwegian Sea and the subpolar North Atlantic compared to the Worthington system, we use temperature assignments slightly different from his, based on our later study of Subpolar Mode Water.

[5] The effect of an alternate cooler temperature for V_{ENT} will be considered later.

Subpolar North Atlantic, lower layer

Volume: $V_{OF} + V_{ENT} - (V_{OF} + V_{ENT}) = 0,$

Heat: $(0.0)V_{OF} + (6.5)V_{ENT} - (2.0)(V_{OF} + V_{ENT}) = 0.$

The lower layer volume equation is an identity, while the other five equations have five unknowns, V_{FSC}, V_{OF}, V_{SPMW}, V_{LSW} and V_{ENT}. Here V_{NPS}, Q_{NS}, and Q_{SPNA} are taken as known quantities, and ρc is taken as nominally 1 cal/(cm^3 °C). These equations are easily manipulated to express V_{FSC}, V_{OF} and V_{ENT} in terms of Q_{NS} and V_{NPS}, and then to express V_{LSW} and V_{SPMW} in terms of Q_{SPNA}, V_{ENT} and V_{FSC}:

$$V_{FSC} = \left(\frac{1}{8.5}\right)\left[\frac{Q_{NS}}{\rho c} + (3.0)V_{NPS}\right]$$
$$= (3.65 + 1.06) \times 10^6 \text{ m}^3 \text{ s}^{-1}$$
$$= 4.7 \times 10^6 \text{ m}^3 \text{ s}^{-1};$$

$$V_{OF} = V_{FSC} - V_{NPS} = \frac{1}{8.5}\frac{Q_{NS}}{\rho c} + \left(\frac{3.0}{8.5} - 1\right)V_{NPS}$$
$$= (4.71 - 3.0) \times 10^6 \text{ m}^3 \text{ s}^{-1}$$
$$= 1.7 \times 10^6 \text{ m}^3 \text{ s}^{-1};$$

$$V_{ENT} = \left(\frac{2}{6.5 - 2.0}\right)V_{OF} = 0.8 \times 10^6 \text{ m}^3 \text{ s}^{-1};$$

$$V_{LSW} = \left(\frac{1}{11.5 - 3.5}\right)$$
$$\times \left[\frac{Q_{SPNA}}{\rho c} - (11.5 - 6.5)V_{ENT} - (11.5 - 8.5)V_{FSC}\right]$$
$$= (10.88 - .48 - 1.77) \times 10^6 \text{ m}^3 \text{ s}^{-1}$$
$$= 8.6 \times 10^6 \text{ m}^3 \text{ s}^{-1};$$

$$V_{SPMW} = \frac{1}{11.5 - 3.5}$$
$$\times \left[\frac{Q_{SPNA}}{\rho c} + (8.5 - 3.5)V_{FSC} + (6.5 - 3.5)V_{ENT}\right]$$
$$= (10.88 + 2.94 + .29) \times 10^6 \text{ m}^3 \text{ s}^{-1}$$
$$= 14.1 \times 10^6 \text{ m}^3 \text{ s}^{-1}.$$

Note that V_{FSC}, V_{OF} and V_{ENT} do not depend in any way on the value of Q_{SPNA}, nor the cyclonic water conversion of the subpolar North Atlantic (see also Figs. 6b, c; 7a, c). The indicated numbers are based on the previously discussed specifications of temperatures and heat fluxes, and on $V_{NPS} = 3.0 \times 10^6$ m^3 s^{-1} (after Worthington, 1970). At both northern and southern boundaries, the transports add up to give a net southward transport of 1×10^6 m^3 s^{-1}. This net transport represents the flow of water from the Pacific Ocean to the Atlantic Ocean via the North Polar Sea.

A comparison of the above results with several other systems is summarized in Table 2. The main differences between the present study (as calculated above) and the Worthington estimates are the less active Norwegian Sea overflows (as anticipated in the introduction), and the active formation of Labrador Sea water in the subpolar basin. While the net warm water flowing northwards past 50°N in eastern North Atlantic is more or less the same, much less of it continues on into the Norwegian Sea, and much more circulates cyclonically in the subpolar North Atlantic. The southward flowing dense water in Worthington's systems at 50°N were totally Norwegian Sea overflows plus entrained warmer waters, while for our system three-fourths of the transport is Labrador Sea water. If the Norwegian Sea heat flux is increased to Worthington's inferred value, then the overflow and Labrador Sea contributions to the dense southward flow are more or less equal. If with our basic system, the colder entrainment temperature of 3.5°C is used rather than 6.5°C, more entrainment is required, the

TABLE 2. Estimation of major current elements (in 10^6 m^3 s^{-1}).

	50°N				Norwegian		Subpolar North Atlantic
	Warm water north	2° water south	3.5°C water south	DWBC (2° + 3.5°)	Warm water north	Dense overflows	Net downwelling (entrainment)
Worthington 1970	13	10	0	10	9	6 (@1°)	4
Worthington 1976	9	6	0	6	9	6 (@1°)	0
Present study	14.1	2.5	8.6	11.1	4.7	1.7 (@0°)	0.8
Present study (high Norwegian Sea heat flux)*	17.1	7.9	6.2	14.1	8.5	5.5 (@0°)	2.4
Present study (cold entrainment)	13.8	4.0	6.8	10.8	4.7	1.7	2.3
Present study (cold entrainment and high Norwegian Sea heat flux)	16.2	12.7	0.4	13.1	8.5	5.5	7.3

* Slightly different Norwegian Sea numbers from Worthington's (1970) on account of slightly different temperature specification and simplification of outflow configuration (contrast Fig. 5 with Fig. 4a).

transport of 2°C water is somewhat increased, and there is less warm water available to convert to Labrador Sea water. For a final, more extreme example, we give a set of estimates using simultaneously Worthington's high Norwegian Sea heat flux value and his low entrainment temperature. The southward flow of 2°C water is maximized for this combination, and there is almost no net Labrador Sea Water—in essence, all the 3.5°C water produced is used for entrainment into the very active V_{OF} to raise its temperature to 2°C.

As a final indication of variability of estimates, the graphs in Figs. 6 and 7 show the response of the system volume fluxes to variation in other specified temperatures, and to prescribed heat fluxes. For reference we have indicated by vertical dashed lines the standard model run described in the above model equation formulation. Dotted lines are provided on the Q_{SPNA} graph to indicate the range of single-year average heat losses for the nine years presented in Bunker's files with full geographic and monthly coverage.

3. Implication of the box model for salinity

The model takes "observed" heat fluxes (calculated by bulk aerodynamic formulas) and the temperatures of inflows and outflows and computes associated volume transports using volume and heat balance equations. In this section we additionally specify the salinities of the inflows and outflows, and deduce the freshwater input into the boxes that is required to satisfy salt conservation, as a small perturbation to the basic model of the previous section. This estimate is then compared with estimates of precipitation, evaporation and run-off.

The procedure for estimating freshwater flux into the boxes is as follows. Such volume fluxes are small

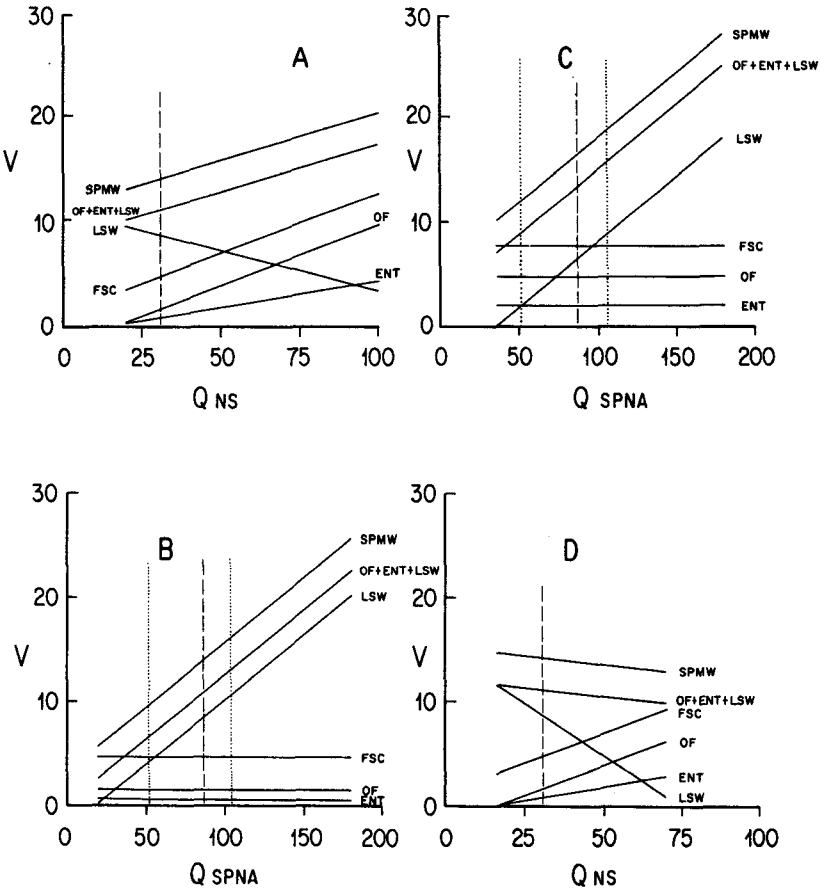

FIG. 6. Examples of the dependence of the water transport rates of the box model on the air–sea heat exchange rate (see text). Units of V are 10^6 m^3 s^{-1}, units of Q are 10^{12} cal s^{-1}. Vertical dashed lines indicate the standard model run discussed in the text. The dotted lines indicate a range of Q_{SPNA} values deduced from the year-to-year variability within the data that makes up the long-term average heat flux reported by Bunker (1976). (A) $Q_{SPNA} = 87 \times 10^{12}$ cal s^{-1}, variable Q_{NS}; (B) $Q_{NS} = 31 \times 10^{12}$ cal s^{-1}, variable Q_{SPNA}; (C) $Q_{NS} = 58 \times 10^{12}$ cal s^{-1} (after Worthington, 1970), variable, Q_{SPNA}; (D) Covariable Q_{NS} and Q_{SPNA}, with $Q_{NS} + Q_{SPNA} = (31 + 87) \times 10^{12}$ cal s^{-1}.

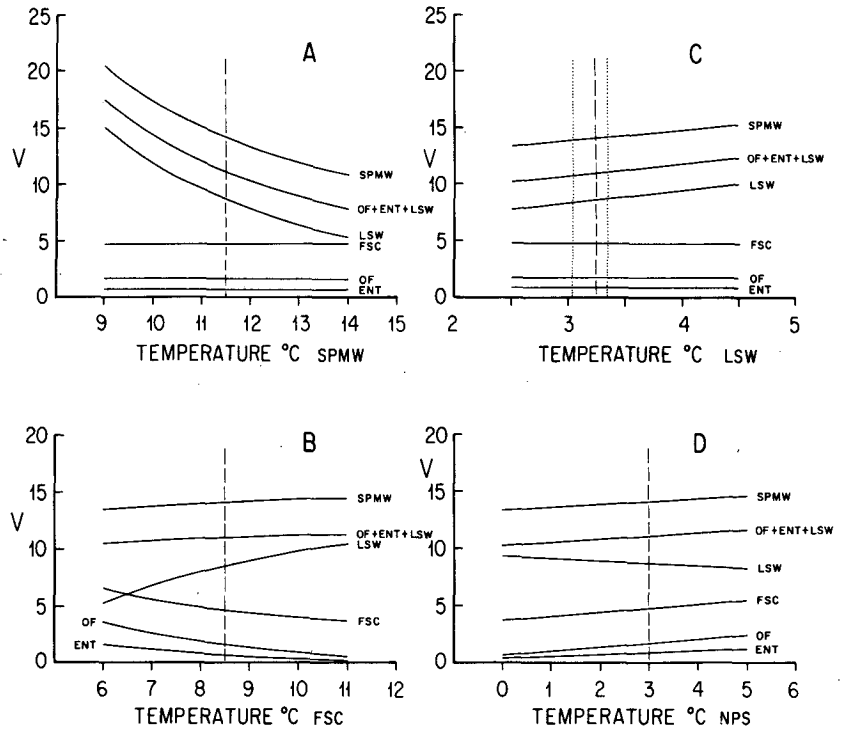

FIG. 7. Examples of the dependence of the water transport rates of the box model on the water mass temperatures. Air–sea heat exchange rates are fixed at the Bunker values $Q_{NS} = 31 \times 10^{12}$ cal s^{-1} and $Q_{SPNA} = 87 \times 10^{12}$ cal s^{-1}. (A) Variable Subpolar Mode Water inflow temperature, (B) Variable Labrador Sea Water outflow temperature. (C) Variable Faroe–Shetland Channel throughflow temperature. (D) Variable North Polar Sea inflow temperature. The vertical dashed lines indicate the standard model run discussed in the text. The vertical dotted lines in panel C indicate the observed range of Labrador Sea Water core temperatures reported by Talley and McCartney (1982), using hydrographic data collected between 1948 and 1975.

and can be ignored in the heat balance equations for each box. In the volume conservation equations, such fluxes appear as small perturbations affecting only the upper layers.

Norwegian Sea

$$V_{FSC} - V_{OF} - V_{NPS} = -\delta$$

with $\delta \ll |V_{NPS}|, |V_{OF}|, |V_{FSC}|$, and a positive value denoting a flux into the box.

Subpolar North Atlantic, upper layer

$$V_{SPMW} - V_{FSC} - V_{ENT} - V_{LSW} = -\epsilon$$

with $\epsilon \ll |V_{SPMW}|, |V_{FSC}|, |V_{ENT}|, |V_{LSW}|$, and a positive value denoting a flux into the box.

In the volume and heat conservation equations, the East Greenland, West Greenland and Labrador Currents are passive, conserving both their volume flux ($V_{GC} = V_{LC}$) and their temperature (0°C). To retain some flexibility in interpreting the freshwater fluxes, we retain in the salinity balance equations the possibility of a salinity change following this current ΔS_{GC} in the Norwegian Sea, and ΔS_{LC} in the Subpolar North Atlantic, with the Δ's defined as positive for salinity increasing following the current downstream. The conservation equations for salt are then

Norwegian Sea

$$S_{FSC}V_{FSC} - S_{OF}V_{OF} - S_{NPS}V_{NPS} = \Delta S_{GC}V_{GC},$$

Subpolar North Atlantic, upper layer

$$S_{SPMW}V_{SPMW} - S_{FSC}V_{FSC} - S_{ENT}V_{ENT} - S_{LSW}V_{LSW} = \Delta S_{LC}V_{LC}.$$

These equations are solved as follows: use the volume equations to express V_{FSC} and V_{SPMW} in terms of the other V_S and, respectively, δ and ϵ. Substitute V_{FSC} and V_{SPMW} into the salt conservation equations to obtain the following:

Norwegian Sea

$$S_{FSC}\delta + \Delta S_{GC}V_{GC} = V_{OF}(S_{FSC} - S_{OF}) + V_{NPS}(S_{FSC} - S_{NPS}),$$

Subpolar North Atlantic, upper layer

$$S_{SPMW}\epsilon + \Delta S_{LC}V_{LC} = V_{FSC}(S_{SPMW} - S_{FSC}) + V_{ENT}(S_{SPMW} - S_{ENT}) + V_{LSW}(S_{SPMW} - S_{LSW}).$$

The right-hand sides of these two equations are positive, and a freshwater input is thus required in each region. There are two mechanisms to supply this freshwater: direct freshwater input (δ and ϵ), representing the excess of precipitation and runoff over evaporation, and the Greenland and Labrador Current systems, which by lateral mixing with the rest of the system may gain salinity downstream (ΔS_{GC} and ΔS_{LC}), or effectively transfer continental runoff to the ocean interior.

The salinities, tabulated in Table 3, are assigned by reference to hydrographic sections and T–S relationships for the various currents. The equations become:

Norwegian Sea

$$35.35\delta + 4\ (\times 10^6\ m^3\ s^{-1})\Delta S_{GC} = 1.22\ (\times 10^6‰\ m^3\ s^{-1}),$$

Subpolar North Atlantic Current

$$35.50\epsilon + (4 \times 10^6\ m^3\ s^{-1})\Delta S_{LC} = 6.66\ (\times 10^6‰\ m^3\ s^{-1}).$$

If the ΔSs are assumed zero, then the total freshwater flux must be supplied by the excess of precipitation and runoff over evaporation, and

$$\delta = 0.035 \times 10^6\ m^3\ s^{-1},$$

$$\epsilon = 0.188 \times 10^6\ m^3\ s^{-1}.$$

These are equivalent to an annual excess of precipitation over evaporation of 33 cm year^{-1} for the Norwegian Sea, and 116 cm year^{-1} for the Subpolar North Atlantic. Baumgartner and Reichel (1975) estimate runoff, precipitation and evaporation for equivalent regions, and their fluxes correspond to 0.038×10^6 m^3 s^{-1} and 0.133×10^6 m^3 s^{-1}. Thus, our estimates of freshwater input appear reasonable.

If, on the other hand, one sets $\delta = \epsilon = 0$, thereby attributing all the freshwater input to the Greenland and Labrador Currents, one obtains $\Delta S_{GC} = 0.31‰$ and $\Delta S_{LC} = 1.67‰$. These salinity changes cannot be ruled out: the Greenland and Labrador Current systems are very stratified in salt, and it is hard to characterize the mean salinity of the current in any given section, let alone decide whether it increases or decreases downstream by a particular amount.

TABLE 3. Salinities of currents (‰).

S_{SPMW}	S_{ENT}	S_{LSW}	S_{FSC}	S_{OF}	S_{NPS}
35.50	35.05	34.85	35.35	34.90	35.20

A last consistency check is the salinity balance in the lower layer of the Subpolar North Atlantic, which has no direct freshwater source. The salt balance is

$$S_{OF}V_{OF} + S_{ENT}V_{ENT} = \bar{S}(V_{OF} + V_{ENT}),$$

where $\bar{S}$ is the mean salinity of the 2°C water flowing southwards at 50°N. Substituting in the numbers from Table 3 and the box model (Table 2, present study) gives $\bar{S} = 34.95‰$, in fair agreement with observation.

In summary, the volume fluxes computed from volume and heat conservation statements and inflow and outflow temperatures are consistent with observed salinities for the same currents, and with estimated levels of freshwater input from precipitation over evaporation, runoff, and lateral exchanges with the relatively fresh Greenland and Labrador Currents. This consistency is not a sharp constraint because of the uncertainties of the lateral exchanges, of open-ocean precipitation levels, and of our volume flux estimates themselves.

4. Concluding remarks

The pycnostad distributions at 50°N described in Section 1 indicate an exchange of water masses between the subtropical and subpolar regions: a northward flow of warm water, dominated by the 11.5°C Mode Water in the east, and a southward flow of the colder products of high-latitude cooling (and freshening) processes. A net northward flow of about 14.1×10^6 m^3 s^{-1} of Subpolar Mode Water and a net southward flow of 15.1×10^6 m^3 s^{-1} of colder water are estimated in the box model (the difference of 1×10^6 m^3 s^{-1} being the net flow from Pacific to Atlantic through the North Polar Sea). The southward flow has three components, two of which are dense and one of which is light. The production of dense components is estimated at about 8.6×10^6 m^3 s^{-1} for Labrador Sea Water and about 2.5×10^6 m^3 s^{-1} for the Norwegian Sea Overflow water (including entrained waters). The light component, the Labrador Current, has been prescribed (not estimated) at 4×10^6 m^3 s^{-1}.

An earlier estimate of Labrador Sea water production was by Wright (1972), for rather different usage. His value of 3.5×10^6 m^3 s^{-1} is still quoted, most recently by Clarke and Gascard (1983). We do not think the physical basis of this estimate is valid. He used an *annual average* heat loss to the atmosphere to support the fall–winter *seasonal* conversion of summer water to winter water. In a local formation model, without an annual average advection of heat into a region, there will be no production. Instead, there will be simply a seasonal cycle of thermocline build-up and erosion (Warren, 1972). To estimate the seasonal conversion of warm water to Labrador Sea Water in such a local formation scheme, the larger fall–winter heat flux should have been used for consistency, but the number will have nothing to do with annual produc-

tion. Another problem is that he has characterized the temperature change by the surface values (8° to 3.5°) rather than the depth-average temperature of the layer involved (more like 5° to 3.5°). The larger the temperature change assumed, the smaller the volume conversion rate, for fixed heat exchange. In any case, one can only support a net annual production of cold water by a lateral advection of heat.

Clarke and Gascard (1983) have produced the ultimate direct estimate: going out in a winter and actually seeing a region of active convective formation and equating the volume observed of new water with the annual production. The equivalent production estimate is 3.9×10^6 m^3 s^{-1}. This seems low compared with our own, but we note the following. Their newly formed Labrador Sea water was an extreme type, of average temperature 3.0°C. If we presume this to be the source water for ordinary Labrador Sea water, it has to mix with its surroundings and increase in temperature. The nearest warm inflow to the region would be the 4°C water of the Irminger Sea (immediately "upstream" in the McCartney and Talley, 1982, cyclonic system, Fig. 1). A volumetric entrainment of an equal part of this water, 3.9×10^6 m^3 s^{-1}, would raise the 3.0° source water to 3.5°C. The total flux of 3.5°C water—traditional Labrador Sea water—would be 7.8×10^6 m^3 s^{-1}. This is quite close to our own estimate.

Our system emphasizes the horizontal cyclonic gyres and the water mass productions following those circulation paths. Our system can be thought of as a meridional circulation cell carrying light water northwards and dense water southwards. The dense water component we estimate at 11.1×10^6 m^3 s^{-1}, a number similar to Worthington's (1970, 1976), although our estimate includes much more Labrador Sea Water.

An estimate of volume transport in the meridional cell using a very different method has been published by Hall and Bryden (1982). They use a hydrographic transect from the Bahamas to Africa at 24°N and published measurements of the Florida Current transport through Florida Straits. Their computations include the net volume transports in layers defined by isotherms (after Worthington, 1976). They estimate the southward flow at temperatures below 4.0°C at 15.6×10^6 m^3 s^{-1} which can be compared with our estimate at 50°N of 11.1×10^6 m^3 s^{-1}. Given the ranges illustrated in Figs. 6 and 7, it is hard to attribute much significance to the difference. It can be rationalized as resulting from continued entrainment following the Deep Western Boundary Current along its southward course from 50 to 24°N.

Roemmich (1980) applied inverse methods to hydrographic sections at 24, 36 and 48°N, with the water column divided into layers by density surfaces. At 24°N, the meridional flow changes sign at $\sigma_\theta = 27.7$ mg cm^{-3} (~5°C) with a net southward transport below that level of $15 \pm 3 \times 10^6$ m^3 s^{-1}, in good agreement with the Hall–Bryden (1982) estimate for the same section. At 36°N the results were similar, while at 48°N, the results were not well-constrained by the method, and ranged from 9 to 25 ($\times 10^6$ m^3 s^{-1}), depending on the initial conditions and constraints used in the inverse calculation.

A larger North Atlantic dataset was used by Wunsch and Grant (1982) for an inverse method analysis of the horizontal circulation patterns and meridional exchanges. Their system, too, used isopycnals to layer the water column. The averages of their estimates for $\sigma_\theta > 27.76$ mg/cm^3 (~4°C) at 48°N and 53°N were, respectively, 14.2×10^6 and 13.0×10^6 m^3 s^{-1}.

These other estimates of volume transports are more direct, using dynamic computations of the horizontal current fields. They are in rough agreement with the indirect estimate of our box model, but generally a little higher. Again, caution must be exercised in attributing any significance to the differences.

The wind-driven, cyclonic circulation has been estimated by Leetmaa and Bunker (1978) at about 40 $\times 10^6$ m^3 s^{-1}. The general level of water mass conversion we have found, 10–15 ($\times 10^6$ m^3 s^{-1}), then implies a thermohaline circulation with magnitude a significant fraction, about 25%, of the subpolar wind-driven gyre. The present box model uses a simple meridional representation of the thermohaline circulation to estimate the intensity of the conversion. It must be kept in mind that this is a two-dimensional representation of a fundamentally three-dimensional system. The horizontal circulation that the meridional cell is superimposed on is discussed in our other papers (McCartney, 1982; McCartney and Talley, 1982; and Talley and McCartney, 1982) and has been schematically represented in Fig. 4c. The main axis of northward flow past 50°N is in the east, and this warm water directly feeds a cyclonic gyre in the Subpolar North Atlantic and indirectly—via a branch through the Faroe–Shetland Channel—a cyclonic gyre in the Norwegian Sea. Air–sea exchanges of heat and freshwater, as well as runoff, cool and freshen the upper water column following these cyclonic advection paths. The end products are the overflow waters for the Norwegian Sea and the Labrador Sea Water for the Subpolar North Atlantic. These products return to subtropical latitudes as deep waters in the western-intensified Deep Western Boundary Current.

Acknowledgments. This work was supported by the Office of Naval Research under Contracts N00014-74-C-0262, NR 083-004 and N00014-79-C-0071, NR 083-004 and by the National Science Foundation under Grant OCE78-22223. The authors wish to express their appreciation to L. V. Worthington for many helpful discussions, to Mary Raymer for her assistance in the analysis and preparation of the materials for this study, and to Karin Bohr for her perseverance in preparing the manuscript.

REFERENCES

Baumgartner, A., and E. Reichel, 1975: *The World Water Balance,* Elsevier, 179 pp.

Bunker, A. F., 1976: Computations of surface energy flux and annual air-sea interaction cycles of the North Atlantic Ocean. *Mon. Wea. Rev.,* **104,** 1122–1140.

——, and R. A. Goldsmith, 1979: Archived time-series of Atlantic Ocean meteorological variables and surface fluxes. WHOI Ref. No. 79-3, Woods Hole Oceanographic Institution, 30 pp.

Clarke, R. A., and J. C. Gascard, 1983: The formation of Labrador Sea Water: Part 1, Large scale processes. *J. Phys. Oceanogr.,* **13,** 1779–1797.

Coachman, L. K., and K. Aagaard, 1974: Physical oceanography of Arctic and subarctic seas. *Marine Geology and Oceanography of the Arctic Seas,* Chap. 1, Springer Verlag, 1–72.

Dietrich, G., 1969: Atlas of the Hydrography of the Northern North Atlantic Ocean. *Cons. Perm. Int. Explor. Mer,* 140 pp.

Hall, M. M., and H. L. Bryden, 1982: Direct estimates and mechanisms of ocean heat transport. *Deep-Sea Res.* **29,** 339–359.

Leetmaa, A., and A. F. Bunker, 1978: Updated charts of the mean annual wind stress, convergences in the Ekman layers, and Sverdrup transports in the North Atlantic. *J. Mar. Res.,* **36,** 311–322.

McCartney, M. S., 1982: The subtropical recirculation of Mode Waters. *J. Mar. Res.,* **40**(Suppl), 427–464.

——, and L. D. Talley, 1982: The Subpolar Mode Water of the North Atlantic Ocean. *J. Phys. Oceanogr.,* **12,** 1169–1188.

Roemmich, D., 1980: Estimation of meridional heat flux in the North Atlantic by inverse methods. *J. Phys. Oceanogr.,* **10,** 1972–1983.

Saunders, P. M., 1982: Circulation in the eastern North Atlantic. *J. Mar. Res.,* **40**(Suppl), 641–657.

Stefánsson, V., 1962: North Icelandic Waters. *Rit. Fiskideilar,* **3,** 269 pp.

Stommel, H., and A. B. Arons, 1960: On the abyssal circulation of the world ocean—I. Stationary planetary flow patterns in a sphere. *Deep-Sea Res.* **6,** 140–154.

Swift, D. J. P., and K. Aagaard, 1981: Seasonal transitions and water mass formation in the Iceland and Greenland Seas. *Deep-Sea Res.* **28,** 1107–1129.

——, —— and S.-A. Malmberg, 1980: The contribution of the Denmark Strait overflow to the deep North Atlantic. *Deep-Sea Res.,* **27,** 29–42.

Talley, L. D., 1984: Meridional heat transport in the Pacific Ocean. *J. Phys. Oceanogr.,* **14,** 231–241.

——, and M. S. McCartney, 1982: Distribution and circulation of Labrador Sea Water. *J. Phys. Oceanogr.,* **12,** 1189–1205.

Warren, B. A., 1972: Insensitivity of subtropical mode water characteristics to meteorological fluctuations. *Deep-Sea Res.,* **19,** 1–19.

Worthington, L. V., 1970: The Norwegian Sea as a mediterranean basin. *Deep-Sea Res.,* **17,** 77–84.

——, 1976: On the North Atlantic circulation. *The Johns Hopkins Oceanography Studies,* No. 6, 110 pp.

Wright, W. R., 1972: Northern sources of energy for the deep Atlantic. *Deep-Sea Res.* **19,** 865–877.

Wunsch, C., and B. Grant, 1982: Towards the general circulation of the North Atlantic Ocean. *Progress in Oceanography,* Vol. 11, Pergamon, 1–59.